ISSN 0965-545X, Polymer Science, Series A, 2016, Vol. 58, No. 5, pp. 825–836. © Pleiades Publishing, Ltd., 2016.
Original Russian Text © N.D. Kondratyuk, G.E. Norman, V.V. Stegailov, 2016, published in Vysokomolekulyarnye Soedineniya, Seriya A, 2016, Vol. 58, No. 5, pp. 519–531.

THEORY AND SIMULATION

Microscopic Mechanisms of Diffusion of Higher Alkanes

N. D. Kondratyuk*, G. E. Norman, and V. V. Stegailov

Joint Institute for Higher Temperatures, Russian Academy of Sciences, Izhorskaya ul. 13, str. 2, Moscow, 125412 Russia
**e-mail: kondratyuk@phystech.edu*

Received December 21, 2015; Revised Manuscript Received March 18, 2016

Abstract—With the use of *n*-triacontane models as examples, abnormal characteristics of diffusion that manifest themselves during the application of the Einstein–Smoluchowski relationship and the asymptotic behavior of velocity autocorrelation function of the molecule-mass centers that is used to calculate the diffusion coefficient via the Green–Kubo formula are investigated. On the basis of the data of complementary approaches, the microscopic mechanisms of diffusion in higher alkanes are outlined. The applicability of the Stokes–Einstein relationship for the viscosity coefficient is demonstrated.

DOI: 10.1134/S0965545X16050072

INTRODUCTION

The transport properties of compounds reflect the specific character of microscopic motion of constituent atoms and molecules. Despite the long history of development of the kinetic theory, which dates back to the work by J.C. Maxwell [1] published in 1860, the exact formulas that make it possible to perform the corresponding calculations of transport coefficients appeared only in the 1950s and were named the *Green–Kubo formulas* [2]. The Green–Kubo formulas are the consequence of the fluctuation–dissipation theorem and express the transport coefficients as time integrals of autocorrelation functions of the corresponding microscopic flows.

The appearance of computers in 1950 made it possible to set the problem of numerical solution of motion equations for systems consisting of many atoms and molecules. Such a theoretical–computational approach was called the *molecular-dynamics method* [3]. Hence, it became possible to calculate the transport properties of almost any compound on the basis of its microscopic description.

Study [4], which was devoted to calculation of a diffusion coefficient for liquid *n*-butane, was the first to utilize the molecular-dynamics method to study the transport properties of liquids of flexible chain molecules. Even this pioneering study showed that the Green–Kubo method gives overestimated values of the diffusion coefficient relative to those given by the Einstein–Smoluchowski method. The problem of agreement between the two equivalent methods has been observed until now, for example, in studies devoted to transfer coefficients of ionic liquids [5, 6]. Many efforts have been made to calculate simple single-atom systems that interact via the Lennard-Jones potential ([7] and references within). For instance, S. Viscardy et al. [7] compared the results of viscosity calculations made via the Green–Kubo formula with the results of calculation of viscosity coefficients directly through the Einstein–Gelfand relationship (an analog of the Einstein–Smoluchowski relation for diffusion). The comparison of viscosity calculations presented a problem because the Gelfand method of moments [8] has not been adopted for a long time for modeling of finite systems under periodical boundary conditions. However, this problem was solved, and as was shown for the case of a Lennard-Jones liquid, the calculations made via the Green–Kubo, Einstein–Smoluchowski, and Einstein–Gelfand equations give equivalent results [7].

There are other methods for prediction of transfer coefficients of *n*-alkane liquids. M.J. Assael et al. [9] presented dependences of diffusion coefficients, viscosity, and thermal conductivity on pressure that were constructed on the basis of molecular-dynamics calculations for the model of solid spheres and the corresponding experimental data. The nonsphericity of *n*-alkane chains is taken into account via the introduction of correction factors independent of temperature and density. P. Blanco et al. [10] interpolated the dependence of the diffusion coefficient in equimolar solutions of *n*-alkanes on the liquid composition over the whole experimental data array.

The model system with the interatomic Lennard-Jones potential is a versatile model for single-atom liquids. The properties of more complex systems are determined by the specific character of the molecular structure and intermolecular interaction. For example, the properties of liquid water are substantially dictated by the dipole moments of molecules and by the possibility to form hydrogen bonds between them. The atomistic models of aqueous systems must take into account these features [11, 12]. With the use of the empirical interatomic potentials, changes in the

hybridization type and cleavage and formation of chemical bonds may be described. In [13], such a reaction potential, AIREBO, was used to simulate the melting of graphite. In [14, 15], the same AIREBO model was applied to study the dynamics of benzene molecules in carbon nanotubes and carbon pores.

This study deals with liquids that consist of high-molecular-mass chain molecules in which intermolecular forces are mainly of the van der Waals nature. An example is the liquid *n*-triacontane (a representative of higher alkanes). P. Padilla and S. Toxvaerd [16, 17] compared the models of united atom with various constants of torsion interactions for *n*-pentane and *n*-decane and showed that, in the case of *n*-alkanes, the diffusion coefficient is strongly affected by intramolecular interactions. In this study, three different models are used to describe intramolecular and intermolecular interactions to characterize the value of a systematic error that is introduced into the calculation results owing to the approximated character of description of interatomic interactions.

Thus, the section Model and the section Calculation Methods present the details of computation of the model of intramolecular and intermolecular interactions, parameters of the computational cell and of the numerical integration of equations for atomic motion, the procedure of the output of the system at equilibrium, and the principles of statistical averaging. The section Self-Diffusion presents the results of calculation of the self-diffusion coefficient according to the Einstein–Smoluchowski equation and via the Green–Kubo formula; it also examines the asymptotics of velocity autocorrelation functions in the considered potentials, compares two methods for the models of liquid *n*-triacontane, and describes the diffusion mechanism specific for higher alkanes. The Section Shear Viscosity presents the estimates of viscosity for the studied system.

MODEL

Interactions in molecular systems can be divided into intramolecular and intermolecular.

The intramolecular part describes interactions between atoms of the same molecule and can be presented as follows:

$$E = E_{\text{bond}} + E_{\text{angle}} + E_{\text{torsion}} + E_{\text{LJ}} + E_{\text{Coul}},$$

where E_{bond}, E_{angle}, and E_{torsion} are valence interactions, such as bonds between the nearest neighbors, and angular and torsion interactions, while E_{LJ} and E_{Coul} are nonvalence interactions, i.e., Lennard-Jones and Coulomb interactions. The first two interactions can be presented in the harmonic form:

$$E_{\text{bond}} = K_b(r - r_0)^2, \quad (1)$$

$$E_{\text{angle}} = K_a(\theta - \theta_0)^2, \quad (2)$$

where K_a and K_b are the energy constants, r and θ are the distance and angle between atoms, and r_0 and θ_0 are the equilibrium values of bond length and angle. The Lennard-Jones interaction is given as (6)–(12)

$$E_{\text{LJ}} = 4\varepsilon[(\sigma/r)^{12} - (\sigma/r)^6], \quad (3)$$

where ε is the interaction constant, σ is the distance at which the interaction energy becomes zero, and r is the distance between atoms. The Coulomb interaction may be written as

$$E_{\text{Coul}} = Cq_iq_j/r, \quad (4)$$

where q_i and q_j are the charges at ith and jth atoms and r is the distance between them.

The torsion interaction has the form $E_{\text{torsion}} = K_{\text{JK}}(1 - \cos[n_{\text{JK}}(\varphi - \varphi^0_{\text{JK}})])$, where K_{JK} is the energy barrier of rotation, n_{JK} is the bond periodicity, φ is the current torsion angle between planes that is set through the corresponding three atoms, and φ^0_{JK} is the equilibrium angle value. The interaction constants depend on the type of chemical environment of the Jth and Kth atoms.

The intermolecular part describes forces that act between atoms of different molecules. These forces are the Lennard-Jones and Coulomb interactions.

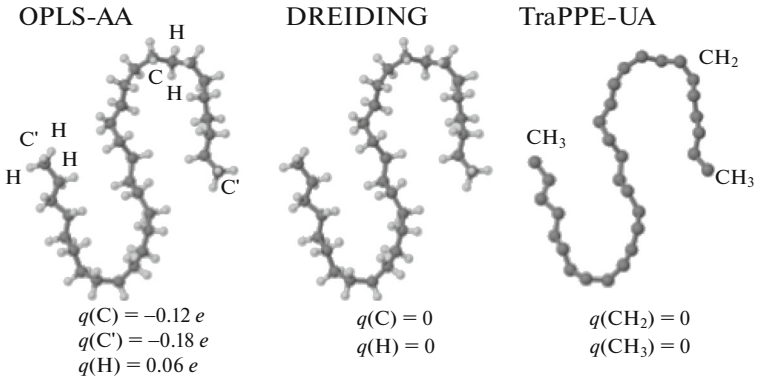

Table 1. Parameters of covalent bonds and angular interactions in the TraPPE-UA, DREIDING, and OPLS-AA potentials

Potential	Bond	K_b, kcal/mol	r_0, Å	Angle	K_a, kcal/mol	θ_0, deg
TraPPE-UA	CH_x–CH_x	268	1.54	CH_x–CH_x–CH_x	62.1	114
DREIDING	C–C	350	1.53	X–C–X	175	109.471
	C–H	350	1.09	″	″	″
OPLS-AA	C–C	268	1.529	C–C–C	58.35	112.7
	C–H	340	1.09	H–C–C	37.50	110.7
				H–C–H	33.0	107.8

Table 2. Parameters of torsion interactions in the TraPPE-UA, DREIDING, and OPLS-AA potentials

Potential	Angle	K_1, kcal/mol	K_2, kcal/mol	K_3, kcal/mol	K_4, kcal/mol
TraPPE-UA	CH_x–CH_x–CH_x–CH_x	1.411	–0.271	3.145	0
DREIDING	X–C–C–X	0	0	0.11111	0
OPLS-AA	H–C–C–H	0	0	0.318	0
	H–C–C–C	0	0	0.366	0
	C–C–C–C	1.740	–0.157	0.279	0

Table 3. Parameters of the Lennard-Jones and Coulomb interactions in the TraPPE-UA, DREIDING, and OPLS-AA potentials

Potential	Atom	ε, kcal/mol	σ, Å	q/e
TraPPE-UA	CH_2	0.0914	3.95	0
	CH_3	0.195	3.75	0
DREIDING	C	0.0951	3.47	0
	H	0.0152	2.85	0
OPLS-AA	C (CH_3)	0.066	3.5	+0.18
	C (CH_2)	0.066	3.5	+0.12
	H	0.03	2.5	–0.06

The DREIDING model [18] (named after Swiss chemist André Dreiding) is a an all-atom model that takes into account all the atoms in the system, where the molecule of *n*-triacontane $C_{30}H_{62}$ is presented in different approaches.

This potential neglects electrostatic interactions. Initially created to investigate the conformations of large molecules, this model is used to predict thermal and mechanical properties of epoxy polymers [19, 20].

The optimized potential for liquid simulations all-atom model (OPLS-AA) [21] is an all-atom potential as well. The difference consists in the fact that parameterization of this model includes the charges of atoms in a molecule and, as a consequence, takes into account the Coulomb interaction. Changes in the distribution of electron density caused by bond polarization are the sources of charges. Carbon atoms have charges of $-0.18e$ (e is the electron charge) in methylene groups (CH_2) and $-0.12e$ in methyl groups (CH_3). Hydrogen atoms bear a charge of $0.06e$. Furthermore, this model has a more complex form of the torsion interaction:

$$2E_{\text{torsion}} = K_1(1+\cos(\varphi)) + K_2(1+\cos(2\varphi)) + K_3(1+\cos(3\varphi)) + K_4(1+\cos(4\varphi)), \quad (5)$$

where K_1, K_2, K_3, and K_4 are the energy constants. OPLS-AA is used to simulate the self-diffusion and structural properties of *n*-alkanes up to *n*-decane [22]. H. Liu et al. [23] used a potential similar to OPLS-AA but having another parameterization to calculate the diffusion coefficients, viscosities, and thermal conductivities of ionic liquids.

The transferable potential for phase equilibria–united atom (TraPPE-UA) [24] is the potential of united atom. The methyl and methylene groups are considered as two effective particles. Positively charged hydrogen atoms are united with negatively charged carbon atoms; as a result, particles are neutral.

In this respect, there is no Coulomb interaction in this model. To set interactions between pseudo atoms, TraPPE-UA uses formulas (1)–(5) with other magnitudes of the parameters. Owing to simplifications related to unification of atoms into groups, the number of interaction constants is reduced and parameterization becomes simpler than that in all-atom considerations. The TraPPE-UA model was used to predict structural and thermodynamic properties of *n*-hexane, *n*-decane, and *n*-heptadecane [25]. The shear viscosities for *n*-decane and *n*-hexadecane were calculated in [26]; the shear viscosities for C_{30} isomers, in [27]. The physical properties of liquid *n*-hexane were investigated in [28]. Similar models, but with other parameters, have been used to investigate the plastic deformation of oligomer glasses (in particular, those consisting of branched alkane $C_{13}H_{31}$) [29], the conformational properties of the liquids $C_{20}H_{42}$ and $C_{48}H_{98}$ [30], and the diffusion of dot structural defects in polymer crystals [31].

Tables 1 and 2 present parameters of covalent, angular, and torsion interactions in the DREIDING, OPLS-AA, and TraPPE-UA models. Table 3 reflects the parameterization of Lennard-Jones and electrostatic interactions.

CALCULATION METHODS

Molecular-Dynamics Method

Calculations were performed via the molecular-dynamics method [32, 33]. The number of molecules in the system varies from 125 to 8000 (to investigate the effect of system size). The size of the computational cell for 125 molecules is 48.38 Å, and that for 8000 molecules is 193.52 Å. The temperature is 353 ± 5 K. Densities in the case of TraPPE-UA and OPLS-AA were 0.77 g/cm^3; densities in the case of DREIDING were 0.69 g/cm^3. The pressure was atmospheric. Periodic boundary conditions were used in calculations. The step in trajectory integration via the molecular-dynamics method was 1 fs. The cutoff radius for electrostatic and Lennard-Jones interactions was 12 Å for all-atom potentials and 14 Å for the TraPPE-UA potential. The long-range part of the Coulomb interaction was calculated via the particle–particle particle–mesh (PPPM) method [34]. Calculations were performed with the LAMMPS molecular-dynamics package [35].

Process of the System Equilibration

For correct calculation of the self-diffusion coefficient, the system must be at equilibrium. Setting the equilibrium configuration in liquids with complex molecules is a nontrivial problem. In addition to the main thermodynamic values (temperature and pressure), the configurational dynamics of molecules during relaxation must be traced. A similar problem may be solved with the use of relative shape anisotropy parameter κ^2, which shows how atoms are located in a molecule relative to the center of mass. It is used to analyze the configurational properties of large molecules [36] and is expressed as $\kappa^2 = \frac{3}{2}\frac{\lambda_1^4 + \lambda_2^4 + \lambda_3^4}{(\lambda_1^2 + \lambda_2^2 + \lambda_3^2)^2} - \frac{1}{2}$, where λ_1, λ_2, and λ_3 are eigenvalues of the inertia tensor of a molecule, $S_{\alpha\beta} = \sum_{i=1}^{N_{\text{atoms}}} m_i(r_i^\alpha - r_{\text{cm}}^\alpha)(r_i^\beta - r_{\text{cm}}^\beta)/m$, where m_i and r_i^α are the mass and coordinate of the *i*th particle in the α direction and m and r_{cm}^α are the mass and coordinate of the center of mass of a molecule in the α direction.

If $\kappa^2 = 1$, all of the atoms of a molecule lie on a single straight line; if $\kappa^2 = 0$, the atoms are located spherically symmetrically relative to the center of mass. When the system is equilibrated the relative shape anisotropy averaged over all the molecules must have a constant value. A similar criterion has been already used to obtain preliminary results [37], but, during this study, the program for calculation of $\langle\kappa^2\rangle$ (averaging over molecules) was substantially improved.

The dependence of $\langle\kappa^2\rangle$ on time during equilibration process in the TraPPE-UA model is presented in Fig. 1. The starting configuration is a gas of identical elongated molecules that are situated at a greater distance than the potential cutoff radius to which $\langle\kappa^2\rangle \sim 1$ corresponds. The velocity distribution that corresponds to 500 K is imparted to molecules. Then, $\langle\kappa^2\rangle$ starts to decrease, a result that testifies that their motion and twisting relative to the center of mass have begun. During compression of the elementary cell to the physical density, the molecules form droplets and are elongated inside them. (The time dependence of density is presented in Fig. 2.) At the next step, the resulting liquid relaxes in the NPT ensemble for 2 ns at atmospheric pressure and 353 K. The average value of density is taken during the last 0.5 ns; at this density, the liquid relaxes in the NVT ensemble for 2 ns. During relaxation of the liquid in the NPT and NVT thermostats, $\langle\kappa^2\rangle$ achieves a constant value and experiences natural fluctuations caused by the dimensions of the cell. This result is evidence that configurational equilibrium occurs in the system. At the last step, the liquid is heated to 700 K for 0.1 ns to decompose metastable states that can form during condensation (because of their length, the molecules can entangle and form coils) and then is thermalized to 353 K. Further calculations are performed for the resulting equilibrium configuration.

The OPLS-AA model utilizes the same mechanism to obtain the equilibrium system, and the density coin-

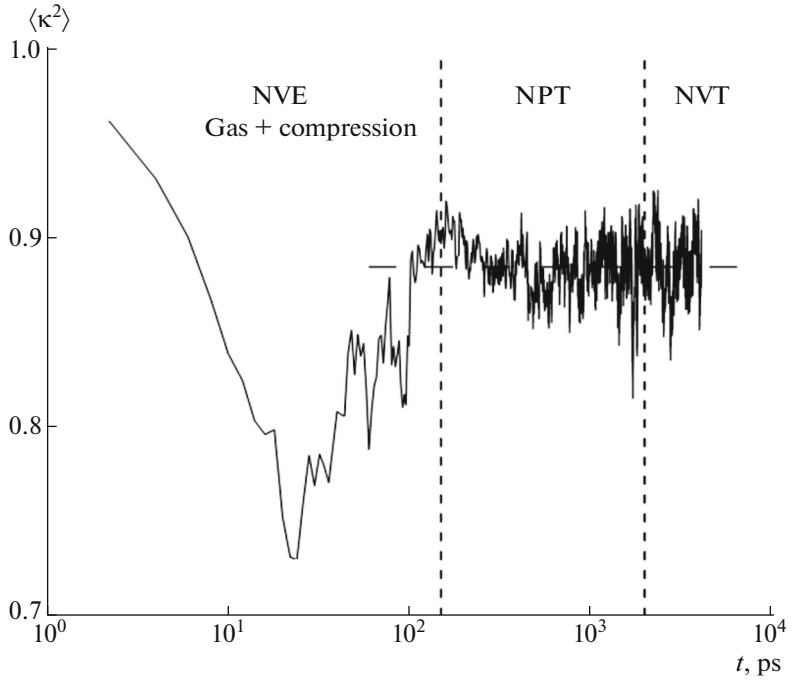

Fig. 1. Dynamics of the averaged relative shape anisotropy $\langle \kappa^2 \rangle$ during the equilibration process in the TraPPE-UA model. See explanations in text.

cides with a good accuracy with the experimental value. In the DREIDING model, under the given conditions, the density during relaxation in the NPT ensemble is 10% lower than the experimental value. From two possible versions of the DREIDING potential (at the experimental density or at atmospheric pressure), we chose the second version, since at the experimental density, the diffusion coefficient is underestimated by approximately an order of magnitude than the experimental one.

Main Relations

The classical method for calculating self-diffusion coefficients is the Einstein–Smoluchowski formula $\langle \Delta r^2 \rangle = 6Dt$, where $\langle \Delta r^2 \rangle$ is the mean-square displacement of the center of mass of a molecule and t is time. Averaging is performed over time and molecules.

The Green–Kubo formulas, which result from the fluctuation–dissipation theorem, are more complex methods for calculating transfer coefficients. For self-diffusion coefficients of liquid molecules, D, the formula has the form

$$D = \int_{t=0}^{\infty} \langle v(0)v(t) \rangle dt/3, \qquad (6)$$

where $\langle v(0)v(t) \rangle$ is the velocity autocorrelation function (VACF) of the center of mass of molecules and t is time.

Statistical Averaging

The results of calculations must be averaged over the molecular-dynamic trajectory. To implement such averaging, the trajectory may be divided into statistically independent regions. The lengths of such regions can be determined from dynamic-memory time t_m. This is the time at the end of which the system forgets its starting conditions. The cause of this phenomenon consists in the fact that the Newton equations for each particle are solved numerically and, as a consequence, differ from the hypothetical accurate solution [3]. The dynamic-memory time can be obtained from the asymptotics of the expressions

$$\begin{aligned} \langle \Delta r^2 \rangle &= \sum_{i=1}^{N} (r_i(t) - r_i'(t))^2/N, \\ \langle \Delta r^2 \rangle &= \sum_{i=1}^{N} (v_i(t) - v_i'(t))^2/N, \end{aligned} \qquad (7)$$

where (r, v) and (r', v') are the trajectories that have the same starting conditions, but are integrable at different time steps. The asymptotics of these expressions have the form $\langle \Delta r^2 \rangle = A\exp(Kt)$ and $\langle \Delta v^2 \rangle = B\exp(Kt)$ when $t < t_m$ and $\langle \Delta r^2 \rangle = 12D(t - t_m)$ and $\langle \Delta v^2 \rangle = 2v_{th}^2$ when $t > t_m$, where D is the diffusion coefficient and $v_{th}^2 = 3k_B T/m$ is the thermal rate.

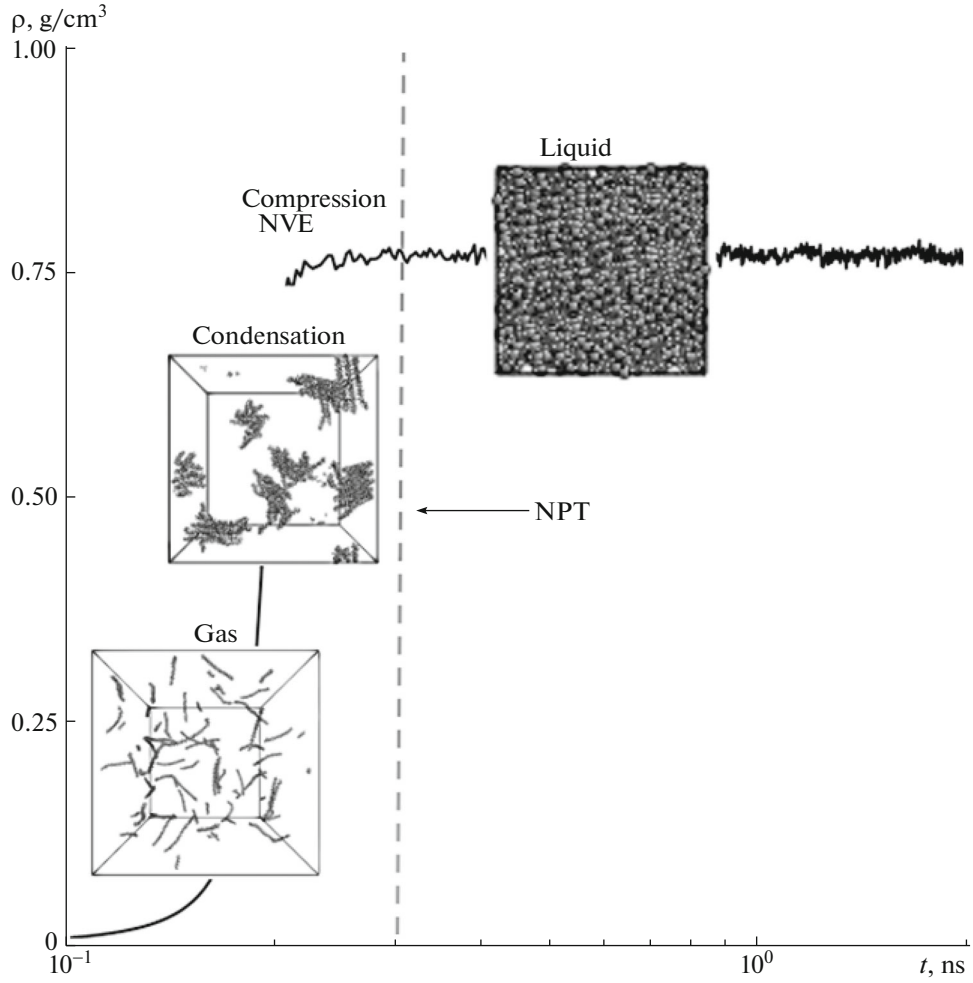

Fig. 2. Dependence of density ρ on time during the process of the system equilibration in the TraPPE-UA model. The inputs depict the characteristic system phases that correspond to the current density.

The calculation of closing errors (7) was performed for the centers of mass of the molecules at integration steps of 0.5 and 1.0 fs. In this system, the memory time is about 3 ps.

The collection of statistics for the VACF is performed via several steps. The first step is classical, $\langle v(0)v(t)\rangle = \sum_{i=1}^{N_{\text{mol}}} v_i(0)v_i(t)/N_{\text{mol}}$, i.e., averaging over molecules. At the second stage, the reference point relative to which $\langle v(0)v(t)\rangle$ is calculated is shifted by a value equal to dynamic-memory time t_{m}: $\langle v(0)v(t)\rangle = \sum_{i=1}^{N_{\text{mol}}} v(t_{\text{m}})v(t_{\text{m}} + t)$. The resulting VACF is the value averaged over all the system molecules and statistically independent reference points.

During calculation of mean-square particle displacement $\langle \Delta r^2 \rangle$, the used averaging method is the same as that in the case of the VACF.

SELF-DIFFUSION

The Einstein–Smoluchowski Formula

The classical dependence (for the Lennard-Jones system) has two power regions: the ballistic region (the starting region, which is caused by the free motion of a molecule without collisions), at which $\langle \Delta r^2 \rangle \sim t^2$ and the diffusion region (caused by the accidental collisions between molecules), at which $\langle \Delta r^2 \rangle = 6Dt$.

The calculation of the self-diffusion coefficient for the centers of mass of molecules in all the three models was performed along a 1-ns trajectory. The computation results are presented in Fig. 3 on the double logarithmic scale to reflect the power dependence of $\langle \Delta r^2 \rangle$ on time. The dotted lines indicate the linear and quadratic dependences.

As in the classical systems, here, the power of the dependence in the initial region is two. In all of the three models, an intermediate region in which the

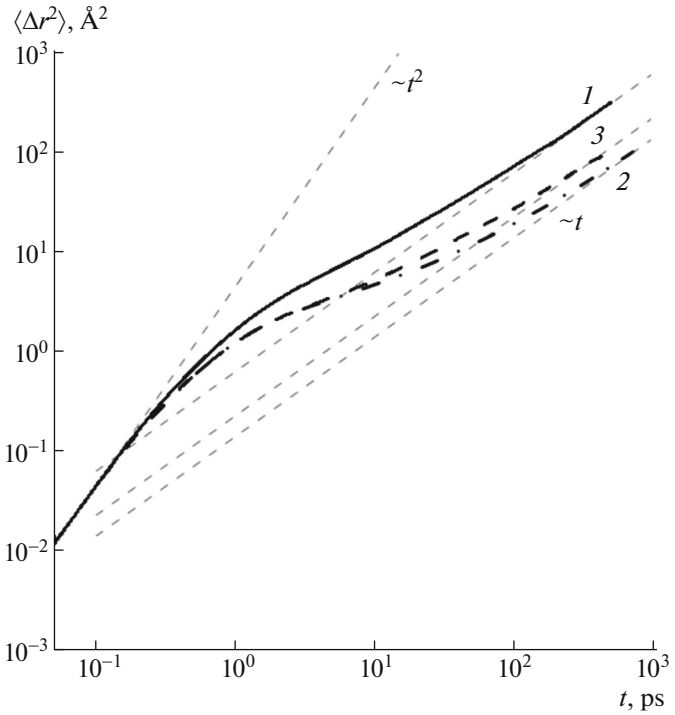

Fig. 3. Dependence of the mean-square displacement of the center of mass on time in the (*1*) TraPPE-UA, (*2*) DREIDING, and (*3*) OPLS-AA models. Gray dotted lines denote the classical asymptotics of ballistic and diffusion modes.

dependence factor is less than unity is observed. In the literature, this region is called the *subdiffusion region* [38]. Similar results were obtained during the molecular-dynamics study of ionic liquids [39] and of the diffusion of monomers in the state with the specific packing pertinent to the disposition of chromatin in eukaryote cell nuclei [40]. It is believed that subdiffusion reflects any difficulties in particle motion [41, 42]. In terms of fractional distributions, for which this mechanism is a special case, diffusion was studied in [43–46]. In the case considered in this study, the deceleration of diffusion of molecules is connected with their length.

To ascertain the character of the subdiffusion region, separate trajectories of the molecules in liquid were investigated. Figure 4 shows a 1-ns trajectory of the center of mass of the system molecules in the DREIDING potential. (The number of molecules in the computational cell is 3375.) The average path of the center of mass of a molecule for such a long time appears to be less than the size of the computational cell (151.14 Å). There are clear regions of localization of the center of mass. The diffusion in such systems has an uneven character with two time scales. The first time scale is caused by disposition inside the localization region. The second is the time of transition from one region to another, and its value can be several orders of magnitude lower. The jumps of positions of the centers of mass of molecules are related to changes in their shape.

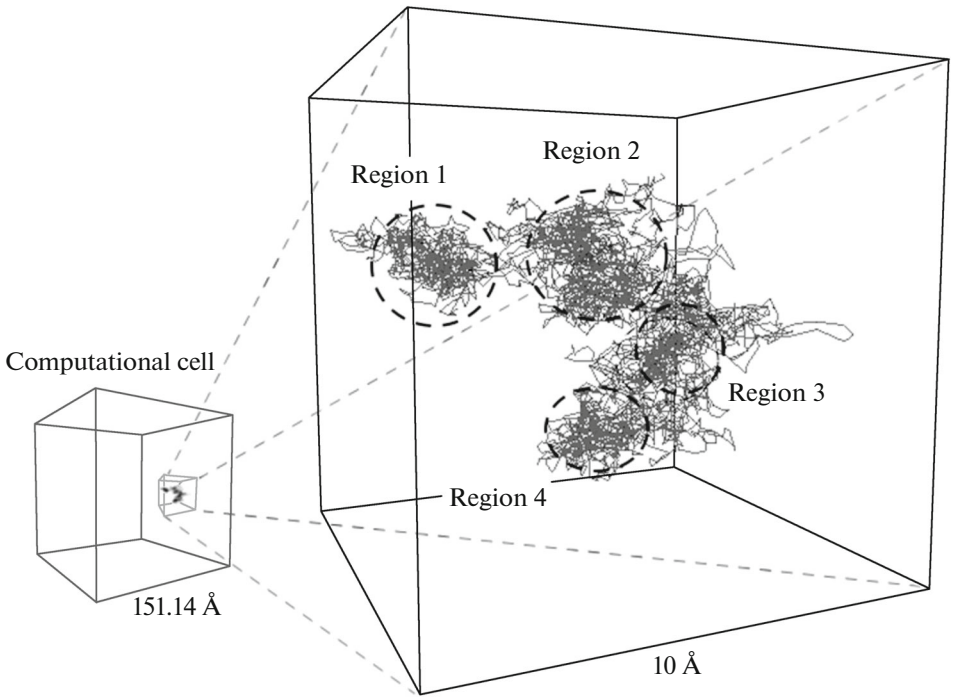

Fig. 4. Dynamics of the center of mass of a molecule in the liquid for 1 ns in the DREIDING model. For scale, the computational cell is depicted in the bottom left corner.

Table 4. Self-diffusion coefficients calculated in various models at 353 ± 5 K and 1 atm

Model	$D_{GK} \times 10^6$, cm^2/s	$D_{ES} \times 10^6$, cm^2/s
TraPPE-UA	5.8 ± 0.6	5.40 ± 0.38
DREIDING	1.5 ± 0.7	1.03 ± 0.07
OPLS-AA	1.74 ± 0.40	1.68 ± 0.12

The experimental value is 2.8×10^{-6} cm^2/s [57].

In the united-atom model, the dependence $\langle \Delta r^2 \rangle(t)$ reaches the linear region, whereas all-atom models require greater times for observation of the diffusion mode. For this purpose, it is necessary to at least double the length of the equilibrium trajectory. Therefore, the self-diffusion coefficients in DREIDING and OPLS-AA at the current stage are calculated from the asymptotic approximations of these dependences. Coefficients D_{ES} that correspond to these asymptotics are presented in Table 4.

The diffusion coefficient in the TraPPE-UA model is higher than that in the all-atom models. The cause of this phenomenon consists in the fact that the molecules are less hindered in motion in the united-atom model because hydrogen is excluded from consideration. Similar effects that are caused by the decreases in certain degrees freedom are discussed in papers devoted to the investigation of large polymer and protein molecules [47, 48].

The effect of system size on the diffusion coefficient during calculation via the Einstein–Smoluchowski method nearly does not manifest itself. Figure 5 shows the results of calculations of the mean-square displacement in the TraPPE-UA model for 125, 1000, and 8000 molecules. In the case of the all-atom potentials DREIDING and OPLS-AA, the dependence remains weak.

The Green–Kubo Formula

The VACFs of centers of mass of molecules normalized to the thermal rate are depicted in Fig. 6 for three models. The length of the calculated trajectory is 1 ns.

In gases and liquids with low densities, the VACF decays to zero asymptotically [49, 50]. In the consideration of ionic clusters in a neutral gas, the oscillations of the VACF associated with ion vibrations are observed [51]. In the current study, VACFs acquire negative values (Fig. 6). The cause of this behavior consists in the fact that, at a certain density, the cases of rebounding collisions of molecules from an effective liquid layer start to predominate over scattering during pair collisions [52]. In this respect, the rate

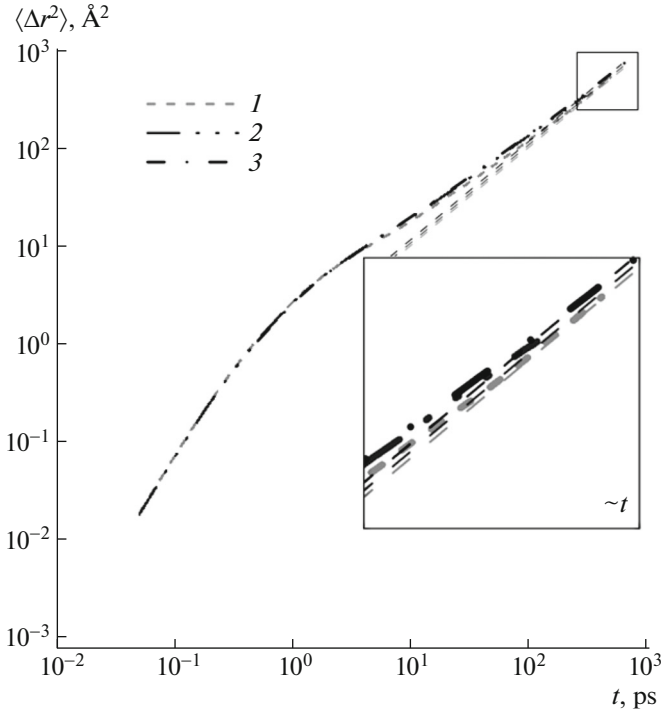

Fig. 5. Dependence of the calculation results for the mean-square displacement of the molecules on the system sizes (the numbers of molecules are (*1*) 125, (*2*) 1000, and (*3*) 8000) in the TraPPE-UA model. The inset is the extended diffusion region.

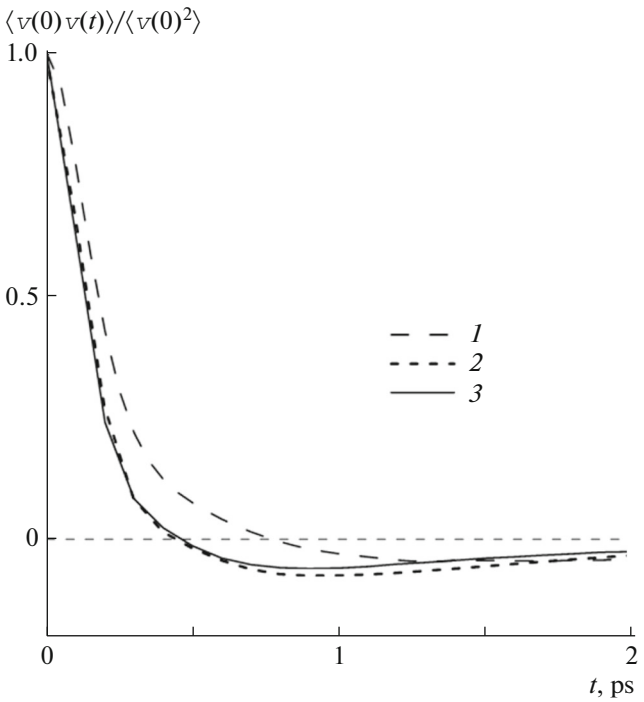

Fig. 6. Normalized velocity autocorrelation functions in the (*1*) TraPPE-UA, (*2*) DREIDING, and (*3*) OPLS-AA models.

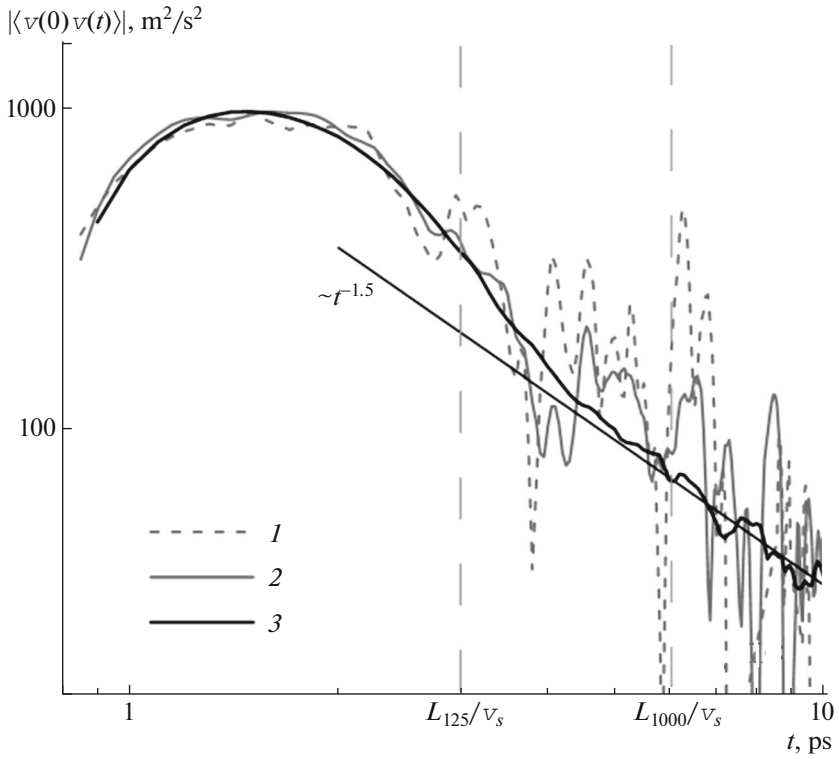

Fig. 7. Dependence of the modulus of the velocity autocorrelation function on the size of the system (the number of molecules are (*1*) 125, (*2*) 1000, and (*3*) 8000) in the TraPPE-UA model.

vector reverses its sign, a circumstance that is reflected in the form of the VACF.

In the united-atom potential TraPPE-UA, for 1 ps, the VACF shows a markedly overrated region, a circumstance that is caused by the features of the model: In the system where hydrogen is excluded from consideration, the centers of mass of the molecules move more freely. This circumstance affects the smoother fading of the VACF. Both all-atom models in the initial region are in good agreement with each other. In this concept, hydrogen atoms promote meshing of liquid molecules and, as a consequence, the VACF decays more rapidly.

An important problem arising in the diffusion studies is the determination of the VACF asymptotics. For example, V.Ya. Rudyak et al. revealed the presence of two exponential regions in the case of diffusion of a lithium nanoparticle in argon [53]. The behavior of the VACF at long times for complex molecules is an important result of the current study.

When the systems of insufficient sizes are considered, a certain analytical dependence at long times cannot be discriminated, owing to the absence of sufficient statistics and to the effect of periodic boundary conditions (Fig. 7). In the calculation with 125 molecules, the velocity correlations are observed up to time L_{125}/v_s (where v_s is estimated through the velocity of sound in alkanes, 1500 m/s), during which the sound wave that arises owing to periodicity has time to cross the system [53, 54]. The calculation for the system with 1000 molecules demonstrates that, along with the boundary conditions, the peculiarities of calculation make contributions. Therefore, to observe the asymptotics, it is necessary to consider large systems including more than 2×10^5 atoms. This value is equivalent to 8000 molecules in the TraPPE-UA model and to 3375 molecules in the all-atom models DREIDING and OPLS-AA.

In the TraPPE-UA model, the transition of the VACF to the power mode $\langle v(0)v(t)\rangle \sim t^{-1.5}$ at 3 ps is clearly seen (Fig. 8). Such an asymptotics has the theoretical foundation for gases and liquids at low densities (when the VACF is strongly positive). The cause of such behavior is the combined motion of liquid molecules [52, 55, 56]. Manifestation of this asymptotics testifies that, in the TraPPE-UA model, the diffusion mechanism is almost the same as the classical mechanism. This fact is confirmed by a relatively insignificant subdiffusion region in the Einstein–Smoluchowski dependence.

Deviations from the classical concept (mode $\langle v(0)v(t)\rangle \sim t^{-2.0}$) are observed in the all-atom approaches (Fig. 8). The existence of localization regions for the centers of mass of molecules deceler-

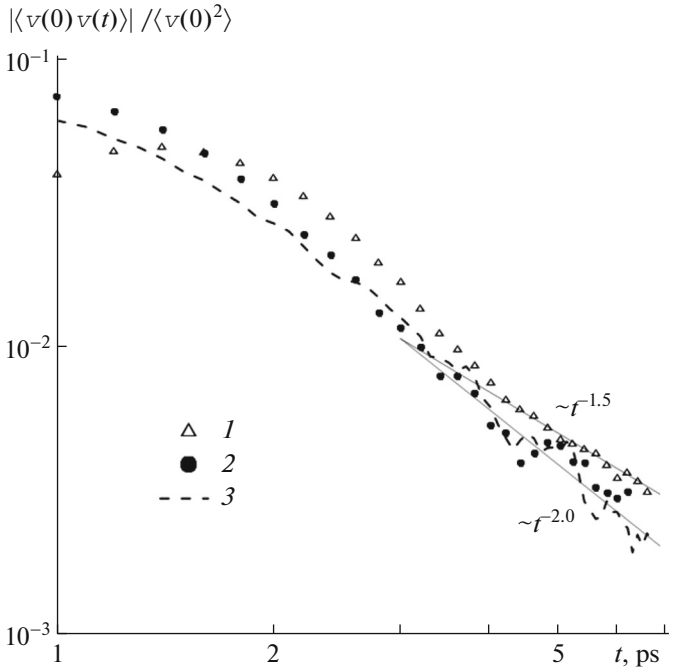

Fig. 8. Asymptotics of the modulus of the normalized velocity autocorrelation function in the (*1*) TraPPE-UA, (*2*) DREIDING, and (*3*) OPLS-AA models. In the TraPPE-UA model, the calculation was performed for 8000 molecules; in the DREIDING and OPLS-AA models, the calculations were performed for 3375 molecules. Gray lines denote the analytical continuations.

ates the diffusion process, a circumstance that is reflected in a more rapid decline of the VACF to zero.

The cutoff of integral (6) has been the key problem for many years and is discussed in many papers dealing with the calculation of transfer coefficients via the Green–Kubo methods. The threshold value to which, from the physical point of view, the integration of the VACF must be performed is time $t_s \sim L/v_s$, but in the case of complex liquids, it is necessary to introduce additional corrections. This problem was faced by the authors of studies [5, 6] during calculation of the diffusion coefficients of ionic liquids: The Green–Kubo method afforded higher values than the Einstein–Smoluchowski relation.

In the simple systems, the asymptotic contribution does not play an important role, because the VACF fades more rapidly than it does in the studied liquid. During neglect of this contribution and the cutoff of the VACF at time L/v_s in the studied liquid, the diffusion coefficient turns out to be 1.5–2 times higher than the value found through the Einstein–Smoluchowski method. For example, in TraPPE-UA in the Green–Kubo method, D_{GK} is 8.41×10^{-6} cm^2/s and $D_{ES} = 5.4\times10^{-6}$ cm^2/s. The situation changes if the contribution of the asymptotic limit of the VACF, D_{Asymp}, is added to the numerical integral, D_{Num}: $D_{GK} = D_{Num} + D_{Asymp}$. In this case, there is better agreement between the methods.

The results of calculations of D_{ES} and D_{GK}, are presented in Table 4 together with the experimental value determined under the specified conditions [57]. In the case of the Einstein–Smoluchowski method, the mentioned errors are statistical (averaging is performed over the independent starting configurations). During calculation via the Green–Kubo method, an error is defined by variation in the VACF asymptotic power because an insignificant change in the parameter entails a fairly substantial change in the value of the corresponding integral. The average values of D_{GK} and error σ_{GK} are calculated from the relationship $D_{GK} = (D_{max} + D_{min})/2$ and $\sigma_{GK} = D_{max} - D_{GK}$, where D_{min} and D_{max} are the minimum and maximum diffusion coefficients, which are defined by the corresponding variations in the power of the analytical continuation of the function.

In the calculation of the diffusion coefficient with the specified precision, the Einstein–Smoluchowski relationship requires a statistics volume several times smaller than that of the Green–Kubo method. This outcome is explained by the fact that such factors as periodic boundary conditions, memory time, and lack of statistics affect determination of the asymptotic limit of the VACF that is used in the Green–Kubo method.

SHEAR VISCOSITY

For a Brownian particle, there is the Stokes–Einstein equation, which connects viscosity η and diffusion coefficient D at given temperature T through particle radius r: $D\eta/kT = 1/6\pi r$.

In the case of polymers, there is a modified relationship based on a series of experimental data and the subsequent theoretical substantiation: $D\eta/k_BT = \rho\bar{h}^2/36M$, where ρ is the density of the considered liquid, $\bar{h}$ is the average distance between the terminal atoms of the molecule, and M is the molecular mass [58].

The viscosity coefficient of *n*-triacontane was estimated through the modified Stokes–Einstein formula because this molecule has an elongated shape and cannot be approximated with a spherical particle. Furthermore, the considered liquid shows peculiarities of diffusion (pertinent to complex systems) that demonstrate the classical relationship is inapplicable to the transfer coefficients.

Length l of the C–C bond in alkanes is about 1.5 Å. The equilibrium angle C–C–C may be taken to be 109.5°, because carbon atoms in alkane molecules have the sp^3 hybridization. Therefore, length L of the molecule in the equilibrium configuration can be rep-

resented as $L = 29l\sin(109.5/2)$. (The skeleton of the molecule consists of 30 carbon atoms.) The value of L is 35.5 Å, accordingly. Average length $\overline{h}$ of the *n*-triacontane molecule in liquid with allowance made for all possible bends lies within the range 20–30 Å.

The viscosity coefficient was estimated at the following parameters: $\rho = 0.77$ g/cm^3, $\overline{h} = 25$ Å, $M = 422.5$ g/mol, $T = 353$ K, and $D = 1.68\times10^{-6}$ cm^2/s (the diffusion coefficient calculated in the OPLS-AA potential). The main contribution to the estimate error is made by determination of the mean distance between the terminal atoms of molecules. If this fact is taken into consideration, it is possible to estimate the relative error of the resulting value: $\sigma_\eta/\overline{\eta} = 2\sigma_h/\overline{h} = 0.4$. In addition, the shear viscosity is 5.5 ± 2.2 mPa s. The experimental value at this temperature is 4.87 mPa s [59].

The fact that the estimate of the viscosity coefficient coincides with the experimental value within the limits of error suggests that the Stokes–Einstein relationship developed for polymers is applicable in the case of higher *n*-alkanes. In addition, this result is evidence for the fact that the classical relationships obtained for the Brownian particles are inapplicable in the case of *n*-alkanes owing to their relatively large length. In the future, the large-scale models of such systems will probably make it possible to refine the models of breakdown phenomena in transformer oils [60, 61].

CONCLUSIONS

The applicability of classical methods to the calculation of diffusion and viscosity coefficients in the case of liquid *n*-triacontane has been studied, and the corresponding diffusion mechanisms have been outlined.

The calculations performed in three different models via the Einstein–Smoluchowski relationship demonstrated that, in the case of long *n*-alkanes, the diffusion mechanism differs from the classical mechanism and that there is a defined subdiffusion region (Fig. 3). This region appearance may be explained by the uneven mechanism of molecule motion, which has two time scales. The first time is related to the disposition of the center of mass of a molecule inside the metastable localization region, and the second time is related to a rapid jump to the adjacent region (Fig. 4). The diffusion coefficient can be found from the linear region of the time dependence of the mean-square displacement of centers of mass.

In the case of complex liquids, the Green–Kubo method is more calculation-consuming than the Einstein–Smoluchowski relationship because the Green–Kubo method requires consideration of large systems to observe the asymptotics of the velocity autocorrelation function (Fig. 7). The analytical contribution of this asymptotics to the integral provides coincidence of the values of the diffusion coefficient in all the models with the values obtained via the Einstein–Smoluchowski relationship within the limits of calculation precision.

The peculiarities of the applied interatomic-interaction model are reflected in the results of calculation of the diffusion coefficient. In the case of the Einstein–Smoluchowski relationship, the dependence $\langle\Delta r^2\rangle(t)$ in TraPPE-UA has almost the classical form (owing to the absence of hydrogen from the system, the molecules move more freely); in all-atom potentials the deceleration of diffusion is expressed owing to hydrogen meshing. During the calculation via the Green–Kubo method, the peculiarities of the approach affect the powers of the VACF asymptotic tails; namely, in all-atom models, the function fades more rapidly.

In this context, the diffusion coefficient in the TraPPE-UA model is overestimated as 5.4×10^{-6} cm^2/s. In the all-atom approaches, the calculated values are closer to the experimental value (2.8×10^{-6} cm^2/s): In the DREIDING and OPLS-AA models, the calculated values are 1.03×10^{-6} and 1.68×10^{-6} cm^2/s, respectively.

The Stokes–Einstein relationship modified for polymers that takes into account effects caused by the molecule length makes it possible to estimate the viscosity of higher *n*-alkanes. The resulting estimate (5.5 ± 2.2 (mPa s)) coincides with the experimental value within the limits of error of the method (4.87 mPa s).

ACKNOWLEDGMENTS

The calculations were performed on the MVS-100K supercomputer of the Interagency Computer Center of the Russian Academy of Sciences.

This work was supported by the Russian Science Foundation, project no. 14-50-00124.

REFERENCES

1. J. C. Maxwell, Philos. Mag. Ser. 4 **19** (124), 19 (1860).
2. M. S. Green, J. Chem. Phys. **22**, 398 (1954).
3. G. E. Norman and V. V. Stegailov, Math. Model. Comput. Simul. **24** (6), 3 (2012).
4. J. P. Ryckaert and A. Bellemans, Chem. Phys. Lett. **30**, 123 (1975).
5. M. H. Kowsari, S. Alavi, M. Ashrafizaadeh, and B. Najafi, J. Chem. Phys. **129**, 224508 (2008).
6. H. Liu, E. Maginn, A. E. Visser, N. J. Bridges, and E. B. Fox, Ind. Eng. Chem. Res. **51**, 7242 (2012).
7. S. Viscardy, J. Servantie, and P. Gaspard, J. Chem. Phys. **126** (18), 1 (2007).
8. E. Helfand, Phys. Rev. **119**, 1 (1960).
9. M. J. Assael, J. H. Dymond, M. Papadaki, and P. M. Patterson, Int. J. Thermophys. **13**, 269 (1992).

10. P. Blanco, M. M. Bou-Ali, J. K. Platten, P. Urteaga, J. A. Madariaga, and C. Santamaria, J. Chem. Phys. **129**, 174504 (2008).

11. C. Vega and J. L. F. Abascal, Phys. Chem. Chem. Phys. **13**, 19663 (2011).

12. G. S. Smirnov and V. V. Stegailov, J. Phys. Chem. Lett. **4**, 3560 (2013).

13. N. D. Orekhov and V. V. Stegailov, Carbon **87**, 358 (2015).

14. Yu. D. Fomin, E. N. Tsiok, and V. N. Ryzhov, J. Comput. Chem. **36** (12), 901 (2015).

15. Yu. D. Fomin, J. Comput. Chem. **34**, 2615 (2013).

16. P. Padilla and S. Toxvaerd, J. Chem. Phys. **95** (1), 509 (1991).

17. P. Padilla and S. Toxvaerd, J. Chem. Phys. **94** (8), 5650 (1991).

18. S. L. Mayo, B. D. Olafson, and W. A. Goddard III, J. Chem. Phys. **101**, 8897 (1990).

19. C. Li and A. Strachan, Polymer **52** (13), 2920 (2011).

20. C. Li, G. A. Medvedev, E. W. Lee, J. Kim, J. M. Caruthers, and A. Strachan, Polymer **53** (19), 4222 (2012).

21. W. L. Jorgensen, D. C. Maxwell, and J. Tirado-Rives, J. Am. Chem. Soc. **118** (45), 11225 (1996).

22. H. Feng, W. Gao, J. Nie, J. Wang, X. Chen, L. Chen, X. Liu, H. Ludeman, and Z. Sun, J. Mol. Model. **19** (1), 73 (2013).

23. H. Liu, E. Maginn, A. E. Visser, N. J. Bridges, and E. B. Fox, Ind. Eng. Chem. Res. **51**, 7242 (2012).

24. M. G. Martin and J. I. Siepmann, J. Phys. Chem. B **102** (14), 2569 (1998).

25. C. Campañá and R. E. Miller, Mol. Simul. **39** (11), 882 (2013).

26. D. A. Hernandez and H. Dominguez, J. Chem. Phys. **138** (13), 134702 (2013).

27. J. D. Moore, S. T. Cui, H. D. Cochran, and P. T. Cummings, J. Chem. Phys. **113** (19), 8833 (2000).

28. R. S. Payal, S. Balasubramanian, I. Rudra, K. Tandon, I. Mahlke, D. Doyle, and R. Cracknell, Mol. Simul. **38** (14–15), 1234 (2012).

29. Al. Al. Berlin, M. A. Mazo, I. A. Strel'nikov, and N. K. Balabaev, Polym. Sci., Ser. D **8** (2), 85 (2015).

30. M. Tsige, J. G. Curro, G. S. Grest, and J. D. McCoy, Macromolecules **36**, 2158 (2003).

31. E. A. Zubova, N. K. Balabaev, and L. I. Manevitch, J. Exp. Theor. Phys. **94** (4), 759 (2002).

32. D. C. Rapaport, *The Art of Molecular Dynamics Simulation* (Cambridge Univ. Press. Sci., Cambridge, 2004).

33. G. E. Norman and V. V. Stegailov, Math. Model. Comp. Simul. **5**, 305 (2013).

34. R. W. Hockney and J. W. Eastwood, *Computer Simulation Using Particles* (Adam Hilger, New York, 1989).

35. S. Plimpton, J. Comput. Phys. **117** (1), 1 (1995).

36. V. Blavatska and W. Janke, J. Chem. Phys. **133** (18), 184903 (2010).

37. N. D. Kondratyuk, G. E. Norman, A. V. Lankin, and V. V. Stegailov, J. Phys.: Conf. Ser **653**, 012107 (2015).

38. O. A. Dvoretskaya, P. S. Kondratenko, and L. V. Matveev, Zh. Eksp. Teor. Fiz. **110** (1), 58 (2010).

39. G. Ivanovskis, G. E. Norman, and D. R. Usmanova, Dokl. Phys. **57** (11), 427 (2012).

40. M. V. Tamm, L. I. Nazarov, A. A. Gavrilov, and A. V. Chertovich, Phys. Rev. Lett. **114**, 178102 (2015).

41. N. F. Fatkullin, G. A. Yatsenko, R. Kimmich, and E. Fisher, J. Exp. Theor. Phys. **87** (2), 294 (1998).

42. D. S. Banks and C. Fradin, Biophys. J. **89** (5), 2960 (2005).

43. V. P. Shkilev, J. Exp. Theor. Phys. **110** (1), 162 (2010).

44. V. P. Shkilev, J. Exp. Theor. Phys. **105** (5), 1068 (2007).

45. V. V. Uchaikin, J. Exp. Theor. Phys. **97** (4), 810 (2003).

46. V. V. Uchaikin, J. Exp. Theor. Phys. **116** (6), 897 (2013).

47. B. Hess, S. Len, N. van der Vegt, and K. Kremer, Soft Matter **2** (5), 409 (2006).

48. V. A. Harmandaris and K. Kremer, Soft Matter **5** (20), 3920 (2009).

49. V. Ya. Rudyak, A. A. Belkin, D. A. Ivanov, and V. V. Egorov, High Temp. **46** (1), 30 (2008).

50. N. M. Chtchelkatchev and R. E. Ryltsev, JETP Lett. **102** (10), 643 (2015).

51. A. V. Lankin, G. E. Norman, and M. A. Orekhov, J. Phys.: Conf. Ser. **653**, 012155 (2015).

52. J. M. Haile, *Molecular Dynamics Simulation, Elementary Methods* (Wiley, Chichester, 1992).

53. V. Ya. Rudyak, S. L. Krasnolutskii, and D. A. Ivanov, Microfluid. Nanofluid **11** (4), 501 (2011).

54. V. Ya. Rudyak, G. V. Kharlamov, and A. A. Belkin, High Temp. **39** (2), 264 (2001).

55. B. J. Alder and T. E. Wainwright, Phys. Rev. A **1** (1), 18 (1970).

56. R. E. Ryltsev and N. M. Chtchelkatchev, J. Chem. Phys. **141**, 124509 (2014).

57. T. Vardag, N. Karger, and H. D. Lüdemann, Ber. Bunsen-Ges. **95** (8), 859 (1991).

58. F. Beuche, J. Chem. Phys. **20**, 1959 (1952).

59. Ch. Wohlfarth and B. Wohlfahrt, *Landolt-Börnstein – Group IV Physical* Chemistry, Vol. 18B: *Pure Organic Liquids* (Springer-Verlag, Berlin, Heidelberg, 2002).

60. M. S. Apfelbaum and E. M. Apfelbaum, J. Electrost. **50**, 129 (2001).

61. M. S. Apfel'baum, Surf. Eng. Appl. Electrochem **45** (2), 102 (2009).

Translated by K. Aleksanyan